

## Calculations of inverse photoemission for jellium models

W. L. Schaich and J. T. Lee

*Department of Physics and Materials Research Institute, Indiana University, Bloomington, Indiana 47405*

(Received 11 April 1991)

Spectra of inverse photoemission are calculated for a jellium model with an image tail on its surface barrier. Various estimates for the spatial variation of the photon field are used in the evaluations with complete matrix elements. An oscillatory structure tied to the vacuum level is found in all spectra and is shown to arise from interference effects in the matrix elements.

Over the last decade inverse photoemission (IPE) has proven to be a valuable probe of electronic states between the Fermi and vacuum levels, as evidenced by a multitude of review articles.<sup>1-11</sup> A typical application of the technique is the study of image states.<sup>2,4-12</sup> These exist as discrete, bound-state solutions of Schrödinger's equation if their energy lies in a gap of the projected band structure for a particular crystal face. When electrons are put into these states, which occur in a Rydberg series just below the vacuum level, they lie primarily outside the metal, trapped in their own image potential well and are incapable of propagating into the metal.

Recently, several authors<sup>13-16</sup> have shown that a remnant of such states can survive in the absence of a gap, i.e., when the electron may freely propagate in the metal. For such cases, which occur on either clean<sup>15,16</sup> or overlayer-covered<sup>13,14</sup> surfaces, one may no longer speak of discrete states but must instead talk of surface resonances. A convenient formalism for this description is based on examining the phase shift suffered by an electron incident from the bulk and scattering off the surface barrier. Since the (normal) energy  $E_n$  is below the vacuum level, the reflection amplitude  $r$  has unit magnitude so we can define a real valued phase shift by  $r = -e^{2i\delta}$ . Standard arguments<sup>17,18</sup> then allow one to relate the energy derivative of  $\delta$  to an incremental surface density of states. The recent calculations have constructed various surface barriers (all with image tails extending out into the vacuum), calculated the phase shift as a function of energy, and found regions of rapid variation of  $\delta(E_n)$ . They deduce that there are resonant peaks in the density of states and assert that these peaks will show up in IPE spectra. Indeed, several cases have been presented where a peak in  $\delta' = d\delta/dE_n$  matches well with experimental data.

In our opinion the last step in the theoretical argument deserves further study, since it is not obvious that  $\delta'$  is the sole, or even dominant, factor for determining an IPE spectrum. The conceptual problem is that eigensolutions exist over a continuous range of energy, and the associated wave functions smoothly change as  $E_n$  varies. It is unclear whether the coupling to these wave functions required by a particular spectroscopic probe should be maximized when  $\delta'$  is at a peak. To settle this question one needs to calculate the appropriate matrix elements. We do that here for the relatively simple jellium model of a clean metal surface.

Our approach exploits the close relationship between

IPE and photoemission.<sup>7,19,20</sup> In a jellium model, where the potential energy only depends on the coordinate normal to the surface (called  $x$ ) and only varies with  $x$  close to the surface, the sole excitation mechanisms are through surface effects and only the  $x$  component of the vector potential can cause transitions. We write the dimensionless IPE yield  $Y$  of photons per incident electron as

$$Y = \int d\Omega_p \int dE^{(l)} \frac{d^2Y}{d\Omega_p dE^{(l)}}, \quad (1)$$

where  $\Omega_p$  describes the solid angle of photon emission and  $E^{(l)}$  the final electron energy. The differential yield is

$$\frac{d^2Y}{d\Omega_p dE^{(l)}} = \frac{\alpha/4\pi^2}{\hbar\omega} \left( \frac{E^{(u)}}{E_n^{(l)}} \right)^{1/2} \left[ |t|^2 \frac{\sin^2\theta_p}{\cos\theta_e} \right] \times |M|^2 \left( \frac{\omega}{kc} \right)^2, \quad (2)$$

where  $\alpha = e^2/\hbar c$  is the fine-structure constant,  $\hbar\omega$  is the photon energy,  $E^{(u)} = \hbar^2 k^2/2m$  is the incident electron energy measured from the vacuum level,  $E_n^{(l)}$  is the final electron energy associated with motion along the normal and measured from the bottom of the (single) bulk band,  $\theta_e$  is the electron angle of incidence, and  $\theta_p$  is the photon angle of exit. The factor in the second set of large parentheses contains the photon angular dependence. The quantity  $t$  is the Fresnel transmission amplitude of the emitted  $p$ -wave photon,

$$t = \frac{2\cos\theta_p}{\epsilon\cos\theta_p + (\epsilon - \sin^2\theta_p)^{1/2}}, \quad (3)$$

where the bulk dielectric function  $\epsilon$  is given by the free-electron expression,

$$\epsilon = 1 - \omega_p^2/\omega^2, \quad (4)$$

with  $\omega_p$  the plasma frequency. Thus just as in photoemission,<sup>21</sup> the photon angular dependence can be made explicit.

The remaining function in (2) is the dimensionless matrix element

$$M = \left\langle \varphi^{(l)} \left| \frac{1}{2} \left[ a \frac{d}{dx} + \frac{d}{dx} a \right] \right| \varphi^{(u)} \right\rangle, \quad (5)$$

where

$$a(x) = \epsilon + \eta(x)(1 - \epsilon) \quad (6)$$

is a scaled form of the normal component of the vector potential. We will evaluate  $M$  for several choices of the complex-valued interpolation function  $\eta$ , which should run from zero in vacuum to one inside the metal. The eigenfunctions in (5) describe only motion along  $x$ . The variation parallel to the surface is given by plane waves, which have already been integrated away. The initial state  $\varphi^{(u)}(x)$  is at energy  $E_n^{(u)} = E^{(u)} \cos^2 \theta_e$  above the vacuum level while the final state  $\varphi^{(l)}(x)$  is at  $E_n^{(l)} = E_n^{(u)} + V_0 - \hbar \omega$  above the band minimum, with  $V_0$  the total barrier height. There is only one final state if  $E_n^{(l)}$  is below the vacuum level, but otherwise there are two orthogonal possibilities.<sup>22</sup> Similarly, since we keep  $\omega < \omega_p / \cos \theta_p$ , there is only one photon final state to consider because the emitted light cannot propagate into the metal.

We have evaluated (2) for several model systems and present results here when the bulk is described by the density parameter  $r_s = 2$ . For the potential energy barrier  $V(x)$  at the surface we use a parametrized form that possesses an image tail.<sup>23</sup> With the parameters of Refs. 24 and 25 this barrier is quite similar near the metal to the self-consistent, local-density-functional barrier of Lang and Kohn.<sup>26</sup> The eigenfunctions are found by a Runge-Kutta integration routine.

There remains the specification of the spatial variation of the perturbing electromagnetic field, i.e., of  $a(x)$  in (6). At the simplest level one can set  $a(x)$  to a constant, which with our emphasis on image states outside the metal we choose to be  $\epsilon$ . The matrix element in (5) can then be reexpressed as

$$M = -\epsilon \langle \varphi^{(l)} | dV/dx | \varphi^{(u)} \rangle / \hbar \omega, \quad (7)$$

which shows that the coupling is strongest where the barrier is most rapidly varying. Alternately, one can use a simple hydrodynamic estimate of  $\eta$ . For  $\omega < \omega_p$  this is written as<sup>27</sup>

$$\eta(x) \approx 1 - e^{-x/d_\perp}, \quad (8)$$

where the origin for  $x$  is at the jellium edge and

$$d_\perp = \frac{\beta/\omega_p}{(1 - \omega^2/\omega_p^2)^{1/2}}, \quad (9)$$

with the spatial dispersion parameter  $\beta = \sqrt{0.6} v_F$ , where  $v_F$  is the (bulk) Fermi velocity. This semiclassical approximation will produce a minimum in the yield at  $\omega_p$ , but is quantitatively unreliable. For a better representation of the electromagnetic field one needs a microscopic evaluation.<sup>28</sup> Here we use the  $\eta$  functions calculated from a random-phase approximation (RPA) treatment of the Lang-Kohn barrier response.<sup>29,30</sup> Results for several frequencies close to  $\omega_p$  are shown in Fig. 1. The strength of the yield scales smoothly with frequency, showing a maximum for  $\omega \approx 0.8\omega_p$  and vanishing at  $\omega_p$ . This resonant behavior in the smooth signal has been seen (and calculated) before.<sup>31</sup> The analogous effect in photoemission was observed some time ago<sup>32,33</sup> and has also been recently reported in electron-energy-loss experiments.<sup>34</sup>

The other striking feature evident in Fig. 1 is an oscillatory structure for final states whose energy of normal

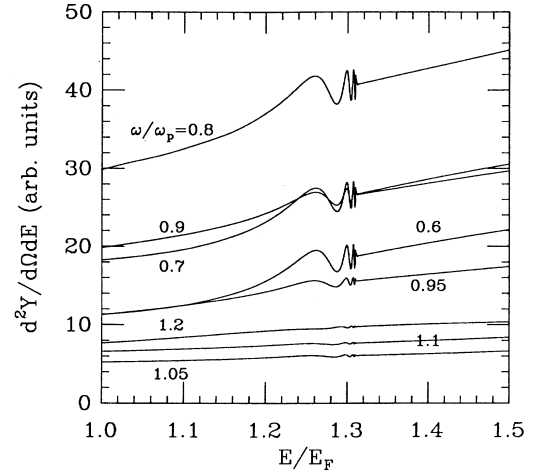


FIG. 1. Differential yields of inverse photoemission at fixed photon energies vs final electron state energy. The electron angle of incidence is  $0^\circ$  and the photon angle of exit is  $45^\circ$ . The bulk jellium has  $r_s = 2$ ; its surface barrier is described by the fitted parameters in Table I of Ref. 24.

motion is just below the vacuum level. This behavior is due to the image tail on the surface barrier. We believe that the structure should be interpreted as arising from interference effects in the excitation matrix elements. To support this claim we show in Fig. 2 how the yield varies at fixed frequency for different choices of the exciting field. The oscillatory pattern is present for each choice of  $a(x)$ , but its strength and location are different. Clearly a peak position cannot be interpreted as a resonance energy, since the same electron states are used for each curve. We

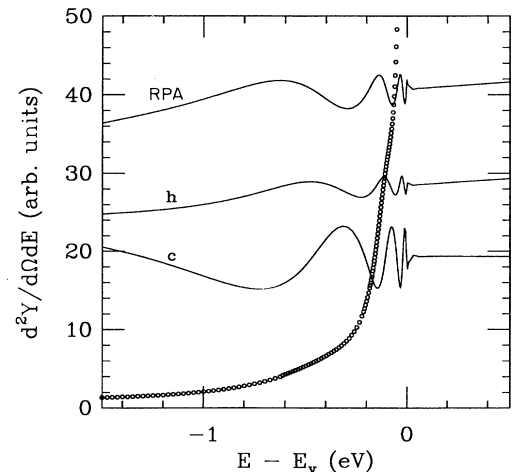


FIG. 2. Different estimates of the differential yield of inverse photoemission vs final electron energy, measured from the vacuum level. The system parameters are the same as in Fig. 1, but the photon energy is fixed at  $\omega/\omega_p = 0.8$  and the various curves have been (differently) scaled for clarity. The RPA result is taken from Fig. 1. The results for hydrodynamic ( $h$ ) and constant ( $c$ )  $a$  functions have been increased by factors of 4 and 100, respectively. The circles show the variation of the extra surface density of states.

also plot a (scaled)  $\delta'$  in Fig. 2 and stress that here the surface density of states does not resemble at all the IPE yields calculated with matrix elements.

The comparison is somewhat more favorable in Fig. 3 where we have repeated the calculations using a less diffuse surface barrier.<sup>15</sup> Now the surface density of states does have clear peaks, but their location and relative strength do not match those from the matrix element calculations, which again move around as the functional form of  $\eta(x)$  is changed. We conclude that  $\delta'$  is not a reliable indicator of the shape of the IPE yield. Note that earlier<sup>15</sup> comparisons with experimental data,<sup>35</sup> which only resolve one maximum, were made with the peak that occurs between 0.4 and 0.5 eV below the vacuum level in Fig. 3.

One can understand the numerical origin of the oscillatory structure by the following qualitative argument. First, we assert that the coupling is spatially localized. This is obvious in (7) due to the appearance of  $dV/dx$ , but also occurs in Eqs. (5) and (6) because of the strong gradients in  $\eta$ , which occur close to the surface. Granting this idea, consider next the wave functions near the surface. The initial state, whose normal energy is well above the vacuum level, is reasonably described by an undeflected WKB wave. Over a small range of  $x$  it appears as a plane wave traveling towards the metal and scaled by a complex amplitude,  $|A|e^{i\varphi}$ , where  $\varphi$  describes the accumulated phase for the electron as it approached the metal. Once inside the metal the amplitude  $|A|$  ceases to change and if the coupling is strongest in this region the influence of  $\varphi$  on  $|M|^2$  cancels out. This argument explains why there is no oscillatory structure in the spectra when both the final and initial states are above the vacuum level.

The difference when the final state lies below the vacuum level is that the surface-barrier reflection amplitude  $r$  then has unit magnitude, rather than being nearly zero. One must consequently view the wave function bound in the metal as a sine wave, rather than as a plane wave. The phase that appears in the argument of this sine function is essentially the  $\delta$  that appears in  $r$ . If the coupling occurs over a small range of  $x$ , there is no way to cancel this phase as argued for states above the vacuum level so  $|M|^2 \sim \sin^2(\delta + \gamma)$  where  $\gamma$  depends on the choice of origin and is a weak function of energy while  $\delta$  diverges as

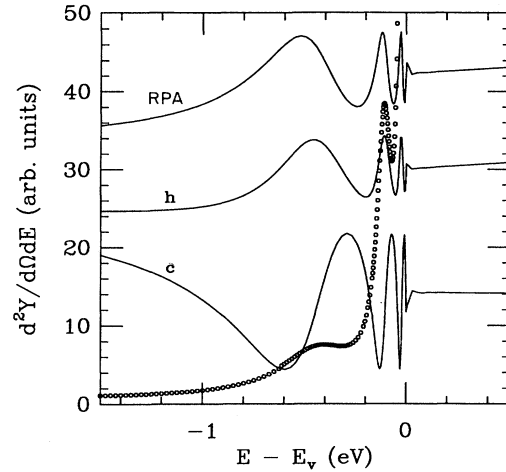


FIG. 3. Same as Fig. 2 except the diffuseness parameter of the surface barrier has been changed from  $\lambda = 1.25$  to  $\lambda = 2.4$ . The  $h$  and  $c$  results have been increased by factors of 4 and 50, respectively.

$E_n^{(l)}$  goes to the vacuum level. This argument explains the "Rydberg series" of interference peaks in all the figures,<sup>36</sup> but cannot give the strength or precise location of the peaks. By concentrating on the behavior of wave functions near the surface, rather than far out in the image tail, it clarifies why nonmonotonic structure in  $\delta$  vs  $E_n$  is not of primary importance, i.e., why peaks in the density of states need not coincide (or even occur) with peaks in IPE. The property should be kept in mind when interpreting experimental data. We remark that a similar modification of interpretation occurred for the threshold structures seen in low-energy electron diffraction.<sup>37-40</sup>

We wish to thank Dr. Paul Bruhwiler for stimulating discussions. Our work was supported in part by the National Science Foundation through Grant No. DMR-89-03851. Some of the calculations were done on the Cray Research, Inc., Y-MP4/464 system at the National Center for Supercomputing Applications at the University of Illinois at Urbana-Champaign (Champaign, IL).

<sup>1</sup>V. Dose, *Prog. Surf. Sci.* **13**, 225 (1983).

<sup>2</sup>N. V. Smith, *Vacuum* **33**, 803 (1983).

<sup>3</sup>F. J. Himpsel and Th. Fauster, *J. Vac. Sci. Technol. A* **2**, 815 (1984).

<sup>4</sup>V. Dose, *Surf. Sci. Rep.* **5**, 337 (1985).

<sup>5</sup>N. V. Smith and D. P. Woodruff, *Prog. Surf. Sci.* **21**, 295 (1986).

<sup>6</sup>F. J. Himpsel, *Comments Condens. Mater. Phys.* **12**, 199 (1986).

<sup>7</sup>G. Borstel and G. Thörner, *Surf. Sci. Rep.* **8**, 1 (1987).

<sup>8</sup>F. J. Himpsel, *J. Phys. Chem. Solids* **49**, 3 (1988).

<sup>9</sup>N. V. Smith, *Rep. Prog. Phys.* **51**, 1227 (1988).

<sup>10</sup>V. Dose, in *Photoemission and Absorption Spectroscopy of Solids and Interfaces with Synchrotron Radiation*, Proceed-

ings of the International School of Physics "Enrico Fermi," Course CVII, edited by M. Campagna and L. Rosei (North-Holland, Amsterdam, 1990), p. 257.

<sup>11</sup>F. J. Himpsel, *Surf. Sci. Rep.* **12**, 1 (1990).

<sup>12</sup>P. M. Echenique and J. B. Pendry, *Prog. Surf. Sci.* **32**, 111 (1989).

<sup>13</sup>S. A. Lindgren and L. Walldén, *Phys. Rev. B* **38**, 10044 (1988).

<sup>14</sup>Lars-Allan Salmi and Mats Persson, *Phys. Rev. B* **39**, 6249 (1989).

<sup>15</sup>S. A. Lindgren and L. Walldén, *Phys. Rev. B* **40**, 11546 (1989).

<sup>16</sup>S. Papadisa, M. Persson, and L.-A. Salmi, *Phys. Rev. B* **41**, 10237 (1990).

- <sup>17</sup>D. Langreth, Phys. Rev. B **5**, 2842 (1972).  
<sup>18</sup>G. Paasch and H. Wonn, Phys. Status Solidi (b) **70**, 555 (1975).  
<sup>19</sup>J. B. Pendry, J. Phys. C **14**, 1381 (1981).  
<sup>20</sup>P. D. Johnson and J. W. Davenport, Phys. Rev. B **31**, 7521 (1985).  
<sup>21</sup>J.-T. Lee and W. L. Schaich, Phys. Rev. B **38**, 3747 (1988).  
<sup>22</sup>W. L. Schaich, in *Photoemission in Solids*, edited by M. Cardona and L. Ley (Springer, New York, 1978), Vol. 1.  
<sup>23</sup>R. O. Jones, P. J. Jennings, and O. Jepsen, Phys. Rev. B **29**, 6474 (1984).  
<sup>24</sup>P. J. Jennings, R. O. Jones, and M. Weinert, Phys. Rev. B **37**, 6113 (1988).  
<sup>25</sup>P. J. Jennings and R. O. Jones, Adv. Phys. **37**, 341 (1988).  
<sup>26</sup>N. D. Lang and W. Kohn, Phys. Rev. B **1**, 4555 (1970).  
<sup>27</sup>W. L. Schaich and K. Kempa, Phys. Scr. **35**, 204 (1987).  
<sup>28</sup>K. Kempa, A. Liebsch, and W. L. Schaich, Phys. Rev. B **38**, 12645 (1988).  
<sup>29</sup>K. Kempa and W. L. Schaich, Phys. Rev. B **37**, 6711 (1988).  
<sup>30</sup>K. Kempa and W. L. Schaich, Phys. Rev. B **39**, 13139 (1989).  
<sup>31</sup>W. Drube, F. J. Himpsel, and P. J. Feibelman, Phys. Rev. Lett. **60**, 2070 (1988).  
<sup>32</sup>H. J. Levinson, E. W. Plummer, and P. J. Feibelman, Phys. Rev. Lett. **43**, 952 (1979).  
<sup>33</sup>P. J. Feibelman, Prog. Surf. Sci. **12**, 267 (1982).  
<sup>34</sup>K.-D. Tsuei, E. W. Plummer, A. Liebsch, K. Kempa, and P. Bakshi, Phys. Rev. Lett. **64**, 44 (1990).  
<sup>35</sup>D. Heskett, K.-H. Frank, E. E. Koch, and M. J. Freund, Phys. Rev. B **36**, 1276 (1987).  
<sup>36</sup>Our calculations have a finite number of peaks because we cut off the image tail at a finite distance from the surface.  
<sup>37</sup>R. E. Dietz, E. G. McRae, and R. L. Campbell, Phys. Rev. Lett. **45**, 1280 (1980).  
<sup>38</sup>J. C. LeBosse *et al.*, J. Phys. C **15**, 3425 (1982).  
<sup>39</sup>R. O. Jones and P. J. Jennings, Phys. Rev. B **27**, 4702 (1983).  
<sup>40</sup>P. J. Jennings and R. O. Jones, Surf. Sci. Rep. **9**, 165 (1988).